

Fractional viscoelastic models: master curve construction, interconversion, and numerical approximation

Samer Wehbe Katicha · G. W. Flintsch

Received: 22 November 2011 / Revised: 29 February 2012 / Accepted: 6 March 2012 / Published online: 1 April 2012
© Springer-Verlag 2012

Abstract We use fractional viscoelastic models that result from the application of fractional calculus to the linear viscoelastic theory to characterize thermorheologically simple linear viscoelastic materials. Model parameters are obtained through an optimization procedure that simultaneously determines the time–temperature shift factors. We present analytical interconversion based on the fractional viscoelastic model between the main viscoelastic functions (relaxation modulus, creep compliance, storage modulus, and loss modulus) and the analytical forms of the relaxation and retardation spectra. We show that the fractional viscoelastic model can be approximated by a Prony series to any desired level of accuracy. This property allows the efficient determination of the fractional viscoelastic model response to any loading history using the well-known recursive relationships of Prony series models.

Keywords Fractional calculus · Time–temperature superposition · Interconversion · Numerical integration · Relaxation time spectrum · Retardation time spectrum · Complex modulus

Introduction

Linear viscoelastic theory describes the behavior of a homogenous, additive, shift invariant causal system. Such a system is mathematically described by convolution of the input with the unit impulse response function to produce the output. In linear viscoelasticity, this convolution is most often written in a slightly different but mathematically equivalent form known as the Boltzmann superposition integral with the stress and strain as input–output pairs (either can be input or output). In general, the kernel of the Boltzmann superposition integral can assume any form as long as it is thermodynamically admissible. Of possible forms, the kernel comprising a sum of exponential functions has received particular interest due to its many desirable characteristics. One such characteristic is that it allows reformulating the linear viscoelastic theory in terms of differential equations with solutions that can be represented in terms of arrangements of springs and dashpots. This formulation provides efficient recursive integration algorithms for linear viscoelastic computations. These algorithms have become the standard in the numerical application of viscoelasticity (e.g., the finite element method).

The weights in the exponential kernel are referred to as the discrete spectrum. In the limit of infinite parameters, the summation is replaced by an integral, which results in the continuous spectrum. In polymer rheology, the continuous spectrum provides insight into the molecular processes occurring at different time scales, which characterize the relaxation process (Stadler and Bailly 2009). The main disadvantage of the exponential kernel is that relaxation of most viscoelastic materials occurs at a slower rate than the decay of exponential

S. W. Katicha (✉) · G. W. Flintsch
Center for Sustainable Transportation Infrastructure,
Virginia Tech Transportation Institute,
Blacksburg, VA, USA
e-mail: skaticha@vtti.vt.edu

G. W. Flintsch
Department of Civil and Environmental Engineering,
Virginia Tech, Blacksburg, VA, USA

functions. For this reason, a large number of exponential functions are needed to provide a good representation of the whole range of response of viscoelastic materials.

During recent times, fractional viscoelastic models have gained wide use in linear viscoelasticity. While fractional viscoelastic models can be traced to the late 1940s (Rossikhin and Shitikova 2010; Mainardi 2010a), most of the currently used approaches follow the work of Caputo and Mainardi (1971). Fractional viscoelastic models initially provided a mathematical description of the relaxation process and were thought to have no physical interpretation. The kernel of these models is the Mittag-Leffler function, which results in a relaxation that asymptotically follows a power-law behavior (Friedrich 1991; Mainardi and Gorenflo 2000). The first successful attempt to provide a physical meaning to fractional models was to show that the Rouse model gives rise to a fractional differential equation of order $1/2$ (Bagley and Torvik 1983). This was further generalized to arbitrary fractional orders (between 0 and 1) by Sharma and Cherayil (2010) who proposed a molecular basis for fractional equations of viscoelasticity in terms of the generalized Langevin equations. The next significant development was establishing the thermodynamic validity of fractional viscoelastic models (Friedrich 1991; Glöckle and Nonnenmacher 1991). The main difference between fractional viscoelastic models and classical viscoelastic models is the replacement of the Newtonian dashpot with the so-called springpot as the dissipative rheological parameter. However, it has been shown that the springpot can be derived from hierarchical and self-similar models comprising springs and dashpots (Schuessel and Blumen 1995; Heymans and Bauwens 1994). Recent efforts have shown that fractional order models arise from the classical generalized Maxwell model (GMM) and generalized Kelvin model (GKM) when the number of elements in these models tend to infinity (Adolfsson et al. 2005; Papoulia et al. 2010).

Until recently, one drawback of fractional viscoelastic models has been the lack of efficient methods for the numerical evaluation of the fractional operator. This results from the fact that at each time step in the discretization of the fractional operator, all strain states from all previous increments are needed to calculate the new strain state (Ford and Simpson 2001; Oeser and Freitag 2009). Different strategies have been proposed to reduce the computational effort of the numerical evaluation of the fractional operator (Enelund and Lesieutre 1999; Padovan 1987; Ford and Simpson 2001; Oeser and Freitag 2009; Adolfsson et al. 2004).

However, these strategies involve approximations that are not easily evaluated and often complicate the problem. To address this, a new strategy based on the approximation of fractional order models with integer order models has been proposed (Papoulia et al. 2010). This allows fractional models to have the computational efficiency of the GMM and GKM while simultaneously maintaining the relatively low number of defining parameters of the corresponding fractional model.

As stated earlier, the spectrum of polymeric materials is often of interest because of its link to molecular processes that govern relaxation. However, direct determination of the relaxation spectrum (or retardation spectrum) from experimental data is an ill-posed problem, and a number of methods based primarily on regularization have been suggested to calculate the discrete spectrum (Mead 1994; Malkin 2006; Stadler and Bailly 2009; Baumgaertel and Winter 1989; Honerkamp and Weese 1989; Kaschta and Schwarzl 1994; Honerkamp and Weese 1993). For this purpose, Friedrich et al. (1995) suggested obtaining the spectrum through analytical inversion of the fractional viscoelastic model. In this case, the spectrum of an n -parameters generalized fractional Maxwell model (GFMM) can be obtained using Laplace transform techniques (Friedrich et al. 1995; Enelund and Lesieutre 1999). Results of analytical inversion performed by Friedrich et al. (1995) compared favorably with results obtained by Honerkamp and Weese (1993) and Weese (1993) for discrete spectrum calculation with nonlinear regularization.

Objective and organization

In this paper, we show how fractional viscoelastic models can be efficiently used to obtain a linear viscoelastic model description from experimental data. Although fractional viscoelastic models have been shown to be able to accurately determine the continuous spectrum (Friedrich et al. 1995), we do not address this issue in this paper. As such, accurate determination of the spectrum is not our objective. Rather, our aim is to obtain a fractional viscoelastic model and show how this model can be used to perform interconversion between viscoelastic functions and to determine the material response under any loading. We provide conditions under which interconversion can be performed analytically and show how fractional viscoelastic models can be approximated by classical rheological models. Given a thermorheologically simple material, the parameters of

the fractional viscoelastic model and time–temperature shift factors are simultaneously obtained during the process of constructing the master curve at a chosen reference temperature. The paper is organized as follows:

In “[Fractional viscoelastic models](#)”, we present a brief overview of fractional calculus and fractional viscoelastic models. Our presentation is concise, and we refer the reader to Mainardi (2010b) and Mainardi and Spada (2011) for a comprehensive presentation of the subject. In Section “[Model determination from dynamic modulus test measurements](#)”, we show how to simultaneously determine the time–temperature shift factors and the fractional viscoelastic model parameters. This essentially entails solving a nonlinear least squares equation. In Section “[Interconversion between the GFMM and the GFKM](#)”, we prove a theorem that states under which conditions exact analytical interconversion of fractional viscoelastic models can be performed. This section builds on results obtained by Koeller (1986). In Section “[Approximation of the GFMM and GFKM by the GMM and GKM](#)”, we show that fractional viscoelastic models can be approximated to any desired level of accuracy by the classical GMM and GKM. This result has been obtained by Adolfsson et al. (2005) and Papoulia et al. (2010). However, the previous authors imposed restrictions on the discretization and limits of integration to prove this assertion. Our approach removes these restrictions and identifies the two sources of errors in the numerical approximation. The first source of error results from approximating an improper integral (an integral that has infinite limits of integration) with a proper integral (an integral that has finite limits of integration). The second source of errors results from approximating a proper integral with a finite summation (i.e., performing numerical integration). An example application using asphalt concrete dynamic modulus test results is presented in Section “[Numerical examples](#)”, and the conclusions are presented in Section “[Conclusion](#)”.

Fractional viscoelastic models

Fractional calculus

Fractional calculus deals with integrals and derivatives of arbitrary (non-integer) order. There are different (i.e., not necessarily equivalent) definitions of frac-

tional operators. The most commonly used operator is the Riemann–Liouville fractional integral operator which associates with a real function $f: P \rightarrow P$, its fractional integral $I_{x_0}^\alpha f$ of order $\alpha > 0$ defined as:

$$I_{x_0}^\alpha f(x) = \frac{1}{\Gamma(\alpha)} \int_{x_0}^x f(\xi) (x - \xi)^{\alpha-1} d\xi \tag{1}$$

Where Γ is the Gamma function and x_0 is an arbitrary fixed point. In what follows, we take $x_0 = 0$ and denote I_0^α by I^α . Note that the Riemann–Liouville fractional integral operator is a generalization of the Cauchy formula for repeated integration defined for the cases when α is a positive integer. Because differentiation is the inverse operator to integration, the fractional derivative can be defined using the integer order derivative with I^α . In this case, there are two possible definitions for the fractional derivative. These are referred to as the left-hand side and right-hand side definitions. The right-hand side definition introduced by Caputo (1967) is referred to as the Caputo derivative and is used in linear viscoelasticity. In general, the Caputo derivative is preferred in physical settings as initial conditions that arise in fractional differential equations are expressed in terms of the function and its integer order derivatives. Another desired property is that the Caputo derivative of a constant is 0. For $\alpha > 0$ and $m - 1 < \alpha < m$, where m is a positive integer, the Caputo (right-hand side) derivative D^α is defined as:

$$D^\alpha f(x) = \frac{1}{\Gamma(m - \alpha)} \int_0^x \frac{d^m f(\xi)}{dx^m} (x - \xi)^{m-\alpha-1} d\xi = I^{(m-\alpha)} \frac{d^m f(x)}{dx^m} \tag{2}$$

The Caputo derivative with $0 < \alpha < 1$ is used to define fractional viscoelastic models. Finally, we note that the fractional integrals and fractional derivatives are linear operators. This is due to their definitions in terms of the classical integer order derivatives and integrals that are linear operators.

Fractional viscoelastic models

In this section, we present the equations of the main viscoelastic functions, namely creep, relaxation, and dynamic functions, that result from fractional viscoelastic models. For a detailed exposition, we suggest the following references: Mainardi (2010b) and Mainardi and Spada (2011). Fractional viscoelastic models result from replacing integer stress and strain derivatives used

in linear viscoelasticity with fractional counterparts. The exponential relaxation function that arises from integer stress and strain derivatives has a short transition zone and is by itself inadequate to describe the relaxation function of real materials. On the other hand fractional models have a long transition zone that depends on the fractional order of differentiation. Therefore, only a few numbers of parameters are needed to describe the relaxation of real materials. The simplest fractional differential equation linking stress σ and strain ε is that of the springpot as described by Koeller (1984):

$$\sigma = E\tau^\alpha D_*^\alpha \varepsilon \tag{3}$$

Where E and τ are the modulus and the relaxation time, respectively. For $\alpha = 0$ the equation represents linear elastic behavior (Hookean spring); for $\alpha = 1$ the equation represents Newtonian viscosity (dashpot). For intermediate values of α , the springpot describes viscoelastic behavior. To describe actual viscoelastic behavior, the springpot is associated in series with at least one elastic element, which gives the fractional Maxwell element. The complex modulus E^* of the fractional Maxwell element as a function of angular frequency ω is shown in Eq. 4 (Heymans 1996; Schiessel et al. 1995).

$$E^*(\omega) = \left(\frac{1}{E} + \frac{1}{E(i\omega\tau)^\alpha} \right)^{-1} = E \frac{(i\omega\tau)^\alpha}{1 + (i\omega\tau)^\alpha} \tag{4}$$

Multiple fractional Maxwell elements and a Hookean spring can be combined in parallel to form the GFMM, which is similar to the GMM that arises from the combination of Maxwell elements. The real (storage modulus) and imaginary (loss modulus) parts of the complex modulus of the GFMM can be obtained by summing the respective moduli of individual fractional Maxwell elements as a result of the fact that the fractional operator is a linear operator.

$$E'(\omega) = E_\infty + \sum_{i=1}^n E_i \frac{(\omega\tau_i)^{2\alpha_i} + (\omega\tau_i)^{\alpha_i} \cos(\alpha_i\pi/2)}{1 + (\omega\tau_i)^{2\alpha_i} + 2(\omega\tau_i)^{\alpha_i} \cos(\alpha_i\pi/2)} \tag{5}$$

$$E''(\omega) = \sum_{i=1}^n E_i \frac{(\omega\tau_i)^{\alpha_i} \sin(\alpha_i\pi/2)}{1 + (\omega\tau_i)^{2\alpha_i} + 2(\omega\tau_i)^{\alpha_i} \cos(\alpha_i\pi/2)} \tag{6}$$

Where E' is the storage modulus, E'' is the loss modulus, and n is the number of fractional Maxwell elements.

The relaxation modulus of the GFMM is calculated using Eq. 7 (Koeller 1984).

$$E(t) = E_\infty + \sum_{i=1}^n E_i \left\{ ML_{\alpha_i} \left[-\left(\frac{t}{\tau_i} \right)^{\alpha_i} \right] \right\} \tag{7}$$

Where,

$$ML_\alpha(x) = \sum_{n=0}^\infty \frac{x^n}{\Gamma(\alpha n + 1)} \tag{8}$$

is the Mittag–Leffler function, a generalization of the exponential function. For the case $\alpha = 1$, the Mittag–Leffler function reduces to the exponential function, and Eq. 7 becomes the Prony series representation of the relaxation modulus.

As the fractional Maxwell element, the fractional Kelvin element comprising a spring combined in parallel with a springpot can be used to obtain the generalized fractional Kelvin model (GFKM). In this case, compliances are easily determined. The creep compliance of the GFKM is calculated as follows:

$$D(t) = D_0 + \sum_{i=1}^n D_i \left\{ 1 - ML_{\alpha_i} \left[-\left(\frac{t}{\lambda_i} \right)^{\alpha_i} \right] \right\} \tag{9}$$

Where $D(t)$ is the creep compliance, D_0 is the initial compliance, D_i is the spring compliance of individual fractional Kelvin elements, and λ_i is the retardation time of individual fractional Kelvin elements. The complex compliance can be obtained from the complex compliance of the single fractional Kelvin element (Schiessel et al. 1995) and that of a single Hookean spring as:

$$D^*(\omega) = D \frac{1}{1 + (i\omega\lambda)^\alpha} \tag{10}$$

The real and imaginary parts of the GFKM are calculated as follows:

$$D'(\omega) = D_0 + \sum_{i=1}^n D_i \frac{1 + (\omega\lambda_i)^{\alpha_i} \cos(\alpha_i\pi/2)}{1 + (\omega\lambda_i)^{2\alpha_i} + 2(\omega\lambda_i)^{\alpha_i} \cos(\alpha_i\pi/2)} \tag{11}$$

$$D''(\omega) = \sum_{i=1}^n D_i \frac{(\omega\lambda_i)^{\alpha_i} \sin(\alpha_i\pi/2)}{1 + (\omega\lambda_i)^{2\alpha_i} + 2(\omega\lambda_i)^{\alpha_i} \cos(\alpha_i\pi/2)} \tag{12}$$

Where D' is the storage compliance and D'' is the loss compliance.

Model determination from dynamic modulus test measurements

For thermorheologically simple materials, the relationship between time and temperature can be described by simple models. For such materials, the effect of changing the temperature is simply to horizontally shift the viscoelastic response as a function of time (or frequency). The time–temperature shift factor $a_T(T)$ is defined as the horizontal shift that must be applied to the response curve measured at an arbitrary temperature T to move it to the curve measured at a chosen reference temperature T_{ref} .

$$a_T = \frac{\tau(T)}{\tau(T_{ref})} \tag{13}$$

For the storage and loss moduli, the horizontal shifting essentially multiplies the frequency of tests performed at a particular temperature by the appropriate shift factor at the particular temperature. For a two parameters GFMM with constant fractional order, this can be expressed as follows:

$$E'(\omega a_T) = E_\infty + \sum_{i=1}^2 E_i \frac{(\omega a_T \tau_i)^{2\alpha} + (\omega a_T \tau_i)^\alpha \cos(\alpha\pi/2)}{1 + (\omega a_T \tau_i)^{2\alpha} + 2(\omega a_T \tau_i)^\alpha \cos(\alpha\pi/2)} \tag{14}$$

$$E''(\omega a_T) = \sum_{i=1}^2 E_i \frac{(\omega a_T \tau_i)^\alpha \sin(\alpha\pi/2)}{1 + (\omega a_T \tau_i)^{2\alpha} + 2(\omega a_T \tau_i)^\alpha \cos(\alpha\pi/2)} \tag{15}$$

To determine the parameters $E_\infty, E_1, E_2, \tau_1, \tau_2, \alpha,$ and $a_T,$ we minimize Eq. 16.

$$\sum_i^{n_f} \sum_{j=1}^{n_T} \{ \log [E'_M(\omega_i, T_j)] - \log [E'_F(\omega_i a_{T_j})] \}^2 + \sum_i^{n_f} \sum_{j=1}^{n_T} \{ \log [E''_M(\omega_i, T_j)] - \log [E''_F(\omega_i a_{T_j})] \}^2 \tag{16}$$

Where n_f and n_T are the number of tested frequencies and temperatures, respectively. The subscripts M and F stand for measured and fractional models, respectively. The minimization is performed with the logarithm of each modulus because the moduli vary across many orders of magnitude. Using the logarithm scale ensures the resulting fit is acceptable for all orders.

Interconversion between the GFMM and the GFKM

Use of the GFMM to calculate the relaxation modulus and use of the GFKM to calculate the creep compliance result from the simplicity of expressing each function in each model. The conversion between the transient responses (relaxation modulus and creep compliance) is more complicated. For example, a constant stress can be applied to the GFMM which results in a creep response. However, the expression of the creep compliance cannot be directly obtained from the GFMM parameters. We know that for the integer order derivative models, the creep compliance expression of an n -parameters GMM is provided by an n -parameters GKM. In this section, we will obtain expressions for the creep compliance of the GFMM and the relaxation modulus of the GFKM. We first state the following theorem:

Theorem *The creep compliance of an n -parameters (with $n > 1$) GFMM with parameters having different fractional order α cannot be expressed in the form of a finite number m -parameters GFKM.*

Proof We first prove the theorem for the case $n = m$. To prove this assertion, we suppose that it is false and show that this leads to a contradiction (a set of incompatible equations). Using the relationship between the creep compliance and the relaxation modulus in the Laplace domain

$$\bar{D}(s) = \frac{1}{s^2 \bar{E}(s)} \tag{17}$$

and the fact that the Laplace transform of the Mittag-Leffler function is expressed by

$$\mathcal{L}\{ML_a(-at^\alpha)\} = \frac{s^{\alpha-1}}{(s^\alpha + a)} \tag{18}$$

we get for an n -parameters GFMM and an n -parameters GFKM, respectively:

$$\bar{E}(s) = E_\infty \frac{1}{s} + \sum_{i=1}^n E_i \frac{s^{\alpha_i-1}}{(s^{\alpha_i} + \tau_i^{-\alpha_i})} \tag{19}$$

$$\bar{D}(s) = \frac{1}{s} \left(D_0 + \sum_{i=1}^n D_i \right) - \sum_{i=1}^n D_i \frac{s^{\alpha_i-1}}{(s^{\alpha_i} + \lambda_i^{-\alpha_i})} \tag{20}$$

Equations 19 and 20 combined with Eq. 17 imply:

$$\frac{\left(D_0 + \sum_{i=1}^n D_i\right) \prod_i \left(s^{\alpha_i} + \lambda_i^{-\alpha_i}\right) - \sum_{i=1}^n D_i s^{\alpha_i} \prod_{j \neq i} \left(s^{\alpha_j} + \lambda_j^{-\alpha_j}\right)}{s \prod_i \left(s^{\alpha_i} + \lambda_i^{-\alpha_i}\right)} = \frac{\prod_i \left(s^{\alpha_i} + \tau_i^{-\alpha_i}\right)}{s \left[E_\infty \prod_i \left(s^{\alpha_i} + \tau_i^{-\alpha_i}\right) + \sum_{i=1}^n E_i s^{\alpha_i} \prod_{j \neq i} \left(s^{\alpha_j} + \tau_j^{-\alpha_j}\right) \right]} \quad (21)$$

For the equality in Eq. 21 to hold we must have (comparing the denominators):

$$\frac{\prod_i \left(s^{\alpha_i} + \lambda_i^{-\alpha_i}\right)}{E_\infty \prod_i \left(s^{\alpha_i} + \tau_i^{-\alpha_i}\right) + \sum_{i=1}^n E_i s^{\alpha_i} \prod_{j \neq i} \left(s^{\alpha_j} + \tau_j^{-\alpha_j}\right)} = \frac{E_\infty + \sum_{i=1}^n E_i}{E_\infty + \sum_{i=1}^n E_i} \quad (22)$$

Expanding both sides of Eq. 22 and equating terms of like powers s^{α_i} , we obtain a set of n equations for $i = 1$ to n that must be satisfied as follows:

$$\prod_{j \neq i} \lambda_j^{-\alpha_j} = \frac{(E_\infty + E_i) \prod_{j \neq i} \tau_j^{-\alpha_j}}{E_\infty + \sum_{i=1}^n E_i} \quad (23)$$

Furthermore, equating the constant term of the expansion of Eq. 22, we obtain (one equation):

$$\prod_j \lambda_j^{-\alpha_j} = \frac{E_\infty \prod_j \tau_j^{-\alpha_j}}{E_\infty + \sum_{i=1}^n E_i} \quad (24)$$

Taking the product of all n equations of Eq. 23 and noting that each term λ_i and τ_i appears $n - 1$ times in this product, we find:

$$\left(\prod_j \lambda_j^{-\alpha_j}\right)^{n-1} = \frac{\prod_j (E_\infty + E_j) \left(\prod_j \tau_j^{-\alpha_j}\right)^{n-1}}{\left(E_\infty + \sum_{i=1}^n E_i\right)^n} \quad (25)$$

Raising Eq. 24 to the $n - 1$ power, we obtain:

$$\left(\prod_j \lambda_j^{-\alpha_j}\right)^{n-1} = \frac{E_\infty^n \left(\prod_j \tau_j^{-\alpha_j}\right)^{n-1}}{\left(E_\infty + \sum_{i=1}^n E_i\right)^{n-1}} = \frac{\left(E_\infty^n + E_\infty^{n-1} \sum_{i=1}^n E_i\right) \left(\prod_j \tau_j^{-\alpha_j}\right)^{n-1}}{\left(E_\infty + \sum_{i=1}^n E_i\right)^n} \quad (26)$$

The left-hand sides of Eqs. 25 and 26 are the same which implies (equating the right-hand side and after simplification) that:

$$\prod_j (E_\infty + E_j) = \left(E_\infty^n + E_\infty^{n-1} \sum_{i=1}^n E_i\right) \quad (27)$$

The equality in Eq. 27 does not hold for arbitrary values of E_∞ and E_j , for $n > 1$. This contradiction proves the theorem for the case of $n = m$. The case $m \neq n$ is trivial as it results in terms of unlike powers. \square

Corollary *The relaxation modulus of n -parameters (with $n > 1$) GFKM with different fractional order α for each parameter cannot be expressed in the form of a finite number m -parameters GFMM.*

Although the interconversion cannot be performed for the GFMM and GFKM comprising fractional Maxwell or Kelvin elements having different fractional orders α , it can be performed if α is restricted to be the same for all model elements. Koeller (1986) provided the conversion of the GFKM to the GFMM for the case of $n = 2$ parameters. Here we give the results for an arbitrary finite number of elements n . The procedure is similar to the interconversion of the classical GMM and GKM ($\alpha = 1$). In this case, we rewrite Eq. 21 and drop the index on α , which results in Eq. 28.

$$\frac{\left(D_0 + \sum_{i=1}^n D_i\right) \prod_i \left(s^\alpha + \lambda_i^{-\alpha}\right) - \sum_{i=1}^n D_i s^\alpha \prod_{j \neq i} \left(s^\alpha + \lambda_j^{-\alpha}\right)}{\prod_i \left(s^\alpha + \lambda_i^{-\alpha}\right)} = \frac{\prod_i \left(s^\alpha + \tau_i^{-\alpha}\right)}{\left[E_\infty \prod_i \left(s^\alpha + \tau_i^{-\alpha}\right) + \sum_{i=1}^n E_i s^\alpha \prod_{j \neq i} \left(s^\alpha + \tau_j^{-\alpha}\right) \right]} \quad (28)$$

Again using the denominators, the parameters λ_i are obtained from the n roots of the n th degree polynomial in s^α given by Eq. 29.

$$\frac{E_\infty \prod_i (s^\alpha + \tau_i^{-\alpha}) + \sum_{i=1}^n E_i s^\alpha \prod_{j \neq i} (s^\alpha + \tau_j^{-\alpha})}{E_\infty + \sum_{i=1}^n E_i} \tag{29}$$

The parameters D_0 and D_i are obtained using the numerators (slightly modified right-hand side numerator) in Eq. 28 as follows:

$$\left(D_0 + \sum_{i=1}^n D_i \right) \prod_i (s^\alpha + \lambda_i^{-\alpha}) - \sum_{i=1}^n D_i s^\alpha \prod_{j \neq i} (s^\alpha + \lambda_j^{-\alpha}) = \frac{\prod_i (s^\alpha + \tau_i^{-\alpha})}{E_\infty + \sum_{i=1}^n E_i} \tag{30}$$

Note that Eq. 24 can also be used to determine GFMM parameters from known GFKM parameters.

Approximation of the GFMM and GFKM by the GMM and GKM

Relaxation and retardation spectra of GFMM and GFKM

The relaxation spectrum is defined in Eq. 31.

$$E(t) - E_\infty = \int_0^\infty \frac{H(\xi)}{\xi} \exp(-t/\xi) d\xi \tag{31}$$

Friedrich et al. (1995) suggested obtaining the spectrum through analytical inversion of the fractional viscoelastic model. In this case, the spectrum of an n -parameters GFMM can be obtained using Laplace transform techniques, which gives (Friedrich et al. 1995; Enelund and Lesieutre 1999):

$$H(t) = \frac{1}{\pi} \sum_{i=1}^n E_i \frac{(t/\tau_i)^{\alpha_i} \sin(\pi \alpha_i)}{1 + 2(t/\tau_i)^{\alpha_i} \cos(\pi \alpha_i) + (t/\tau_i)^{2\alpha_i}} \tag{32}$$

Where $\sum_{i=1}^n E_i = E_0 - E_\infty$

To obtain the retardation spectrum we start from its definition given in Eq. 33:

$$D(t) - D_0 = \int_0^\infty \frac{L(\xi)}{\xi} [1 - \exp(-t/\xi)] d\xi \tag{33}$$

For the case of a single parameter GFKM, Eq. 33 can be written as

$$D_1 \left\{ 1 - ML_\alpha \left[- \left(\frac{t}{\lambda} \right)^\alpha \right] \right\} = \int_0^\infty \frac{L(\xi)}{\xi} [1 - \exp(-t/\xi)] d\xi \tag{34}$$

$$D_1 - D_1 ML_\alpha \left[- \left(\frac{t}{\lambda} \right)^\alpha \right] = \int_0^\infty \frac{L(\xi)}{\xi} d\xi - \int_0^\infty \frac{L(\xi)}{\xi} \exp(-t/\xi) d\xi \tag{35}$$

We note that the left-hand side and the right-hand side of Eq. 35 comprise of one time-dependent and another time-independent term. For the equation to be valid, it has to be satisfied term by term; that is:

$$D_1 = \int_0^\infty \frac{L(\xi)}{\xi} d\xi \tag{36}$$

$$D_1 ML_\alpha \left[- \left(\frac{t}{\lambda} \right)^\alpha \right] = \int_0^\infty \frac{L(\xi)}{\xi} \exp(-t/\xi) d\xi \tag{37}$$

Equation 37 is similar to Eq. 31. Therefore, the retardation spectrum of an n -parameters GFKM can be obtained using the same procedure as the one used to obtain the relaxation spectrum of the GFMM, which gives:

$$L(t) = \frac{1}{\pi} \sum_{i=1}^n D_i \frac{(t/\lambda_i)^{\alpha_i} \sin(\pi \alpha_i)}{1 + 2(t/\lambda_i)^{\alpha_i} \cos(\pi \alpha_i) + (t/\lambda_i)^{2\alpha_i}} \tag{38}$$

Discrete relaxation and retardation spectra and Prony series parameters

For the fractional viscoelastic model, the integral in Eq. 31 can be performed analytically (it basically results in the Mittag–Leffler function). There are, however, advantages to obtaining a numerical approximation of the integral. This numerical approximation gives the Prony series approximation to the GFMM. In this section, we show that the Prony series approximation converges to the GFMM. This means that the GFMM can be

represented to any level of desired accuracy by a finite Prony series expansion. The Prony series formulation has the advantage of providing a convenient recursive integration algorithm for linear viscoelastic computation. The computational effort in the recursive integration is proportional to the number of terms in the Prony series expansion (Taylor et al. 1970) and only requires storing the stress and strain values from the previous time step. This has led to its adoption in nonlinear viscoelasticity to computations involving the Schapery nonlinear viscoelastic material model (Henriksen 1984; Roy and Reddy 1988; Lai and Bakker 1996; Haj Ali and Muliana 2004). On the other hand, available methods for the numerical evaluation of the fractional operator are slow as at each time step all strain states from all previous increments are needed to calculate the new strain state (Ford and Simpson 2001; Oeser and Freitag 2009).

Papoulia et al. (2010) and Adolfsson et al. (2005) proved that the integral in Eq. 31 under certain restrictions placed on the discretization could be approximated by a Prony series expansion. We present an alternative proof that removes these restrictions and is in our opinion significantly shorter and simpler than the proof provided by Papoulia et al. (2010). The simplicity follows from recognizing that the approximation involves two steps. The first step approximates an improper integral (one with infinite limits of integration) using a proper integral (one with finite limits of integration). The second step approximates the proper integral with a Riemann sum. We start with Eq. 39, which is equivalent to Eq. 31.

$$g(t) = E(t) - E_\infty = \lim_{b \rightarrow \infty} \int_0^b \frac{H(\xi)}{\xi} \exp(-t/\xi) d\xi$$

$$= \lim_{b \rightarrow \infty} \int_0^b f(\xi) d\xi \tag{39}$$

Where g and f are introduced to simplify the notation. Since the limit in Eq. 39 exists (because it gives the fractional viscoelastic model), we find by the definition of the limit that for every $\varepsilon > 0$ there exists a c (in this case $c > 0$) such that

$$\left| g(t) - \int_0^b f(t, \xi) d\xi \right| < \frac{\varepsilon}{2} \tag{40}$$

whenever $b > c$. This asserts that we can come arbitrarily close to the value of the improper integral, $g(t)$, if we

make b large enough. Furthermore, because $f(\xi) > 0$ for all $\xi > 0$,

$$\left| g(t) - \int_0^{b_2} f(t, \xi) d\xi \right| < \left| g(t) - \int_0^{b_1} f(t, \xi) d\xi \right| \tag{41}$$

for all $b_2 > b_1$. Equation 41 shows that the approximation error strictly decreases with increasing b . Now $f(\xi)$ is continuous on $[0, b]$ except at $\xi = 0$. However, we have

$$\lim_{\xi \rightarrow 0} f(t, \xi) = \lim_{\xi \rightarrow 0} \frac{\exp(-t/\xi)}{\pi} \sum_{i=1}^n \times E_i \frac{(\xi/\tau_i)^{\alpha_i} \sin(\pi\alpha_i)}{1 + 2(\xi/\tau_i)^{\alpha_i} \cos(\pi\alpha_i) + (\xi/\tau_i)^{2\alpha_i}} = 0 \tag{42}$$

Therefore, we can make f continuous at every point in $[0, b]$ by setting $f(t, 0) = 0$. Under these conditions, the function f has a Riemann integral. Using Theorem 6.8 in Rudin (1976), we can find $\delta > 0$ and $\varepsilon > 0$ such that any partition $P = [\xi_0, \xi_1, \dots, \xi_n]$ of $[0, b]$ with $\Delta\xi_i < \delta$ for all i implies

$$U(P, f) - L(P, f) < \frac{\varepsilon}{2} \tag{43}$$

Where $U(P, f)$ and $L(P, f)$ are the upper and lower Riemann sums of f over $[0, b]$, respectively. Furthermore, conditions stated in Theorem 6.7 (b) of Rudin (1976) are met, and we have that

$$\left| \sum_{i=1}^n f(t, \xi_i) \Delta\xi_i - \int_0^b f(t, \xi) d\xi \right| < \frac{\varepsilon}{2} \tag{44}$$

for any arbitrary point in $[\xi_{i-1}, \xi_i]$. We can now write

$$\left| g(t) - \sum_{i=1}^n f(t, \xi_i) \Delta\xi_i \right| = \left| g(t) - \int_0^b f(t, \xi) d\xi + \int_0^b f(t, \xi) d\xi - \sum_{i=1}^n f(t, \xi_i) \Delta\xi_i \right|$$

$$\leq \left| g(t) - \int_0^b f(t, \xi) d\xi \right| + \left| \sum_{i=1}^n f(t, \xi_i) \Delta\xi_i - \int_0^b f(t, \xi) d\xi \right| < \frac{\varepsilon}{2} + \frac{\varepsilon}{2} = \varepsilon \tag{45}$$

which shows that the improper integral, $g(t)$, can be approximated to any desired level of accuracy by the finite sum given the appropriate c and δ . In the numerical examples presented later, we illustrate how c and δ affect accuracy. With the approximation of the integral, the relaxation modulus then becomes

$$E(t) \approx E_\infty + \sum_{i=1}^n f(t, \xi_i) \Delta \xi_i \tag{46}$$

$$E(t) \approx E_\infty$$

$$+ \sum_{i=1}^n \left(\frac{1}{\pi} \sum_{j=1}^m E_j \frac{(\xi_i/\tau_j)^{\alpha_j} \sin(\pi \alpha_j)}{1 + 2(\xi_i/\tau_j)^{\alpha_j} \cos(\pi \alpha_j) + (\xi_i/\tau_j)^{2\alpha_j}} \right) \times \frac{\Delta \xi_i}{\xi_i} \exp(-t/\xi_i) \tag{47}$$

Where n is the number of Prony series parameters and m is the number of fractional Maxwell elements in the GFMM. Equation 47 is the Prony series representation of the relaxation modulus with Prony series coefficients given by Eq. 48.

$$C_i = \left(\frac{1}{\pi} \sum_{j=1}^m E_j \frac{(\xi_i/\tau_j)^{\alpha_j} \sin(\pi \alpha_j)}{1 + 2(\xi_i/\tau_j)^{\alpha_j} \cos(\pi \alpha_j) + (\xi_i/\tau_j)^{2\alpha_j}} \right) \frac{\Delta \xi_i}{\xi_i} \tag{48}$$

In Adolfsson et al. (2005) the parameters C_i were determined from a uniform distribution on a linear time scale. In this case, the convergence of the Prony series expansion to the fractional model was slow (with data

spanning only three decades and use of 1,000 Prony series parameters the difference between the Prony series and the fractional relaxation modulus is still visually noticeable in a plot). The convergence can be significantly improved using a uniform distribution on a logarithmic time scale and rewriting Eq. 31 in the form presented in Eq. 49.

$$E(t) - E_\infty = \int_{-\infty}^{\infty} H(\ln \xi) \exp(-t/\ln \xi) d \ln \xi \tag{49}$$

In this case, Prony series parameters are given by Eq. 50.

$$C_i = \left(\frac{1}{\pi} \sum_{j=1}^m E_j \frac{(\xi_i/\tau_j)^{\alpha_j} \sin(\pi \alpha_j)}{1 + 2(\xi_i/\tau_j)^{\alpha_j} \cos(\pi \alpha_j) + (\xi_i/\tau_j)^{2\alpha_j}} \right) \Delta \ln \xi_i \tag{50}$$

Numerical examples

We present a numerical example using the fractional viscoelastic model to determine linear viscoelastic properties of asphalt concrete. Asphalt concrete is considered thermorheologically simple, and the GFMM is simultaneously determined with the time–temperature shift factors using asphalt concrete dynamic complex modulus test results at different temperatures and frequencies to construct the dynamic modulus master curve. From the GFMM we obtain the GFKM and use the norm of dynamic complex moduli of both models

Fig. 1 Measured storage and loss moduli

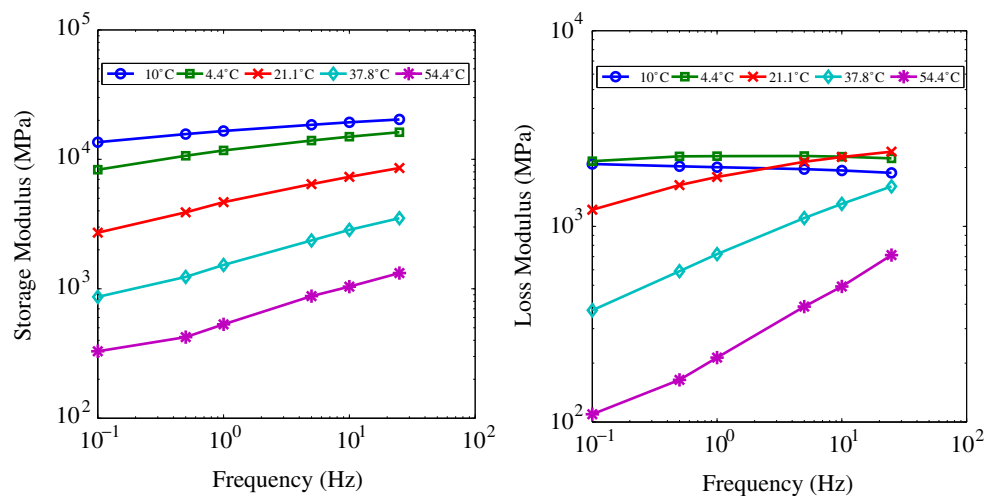
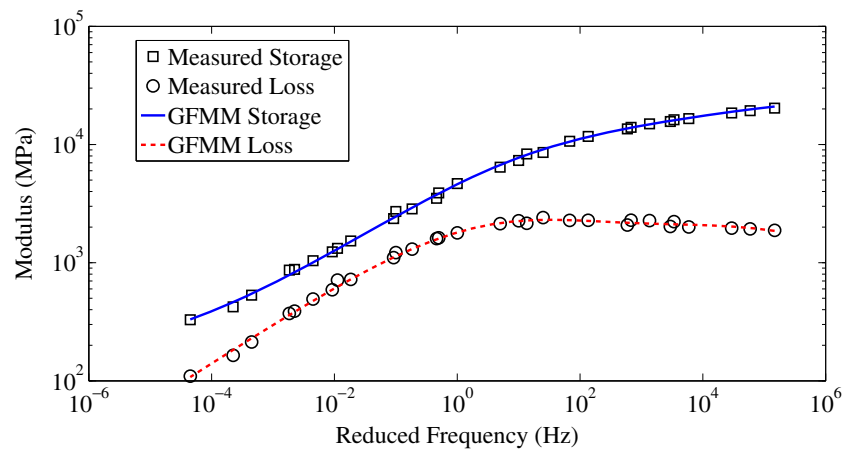


Fig. 2 Storage modulus and loss modulus master curves



to evaluate the accuracy of our calculation. We then obtain the continuous and discrete relaxation spectra and evaluate the sources of errors that result in approximating the integral in Eq. 31 with a Prony series expansion.

Asphalt concrete dynamic modulus master curve construction

The construction of the asphalt concrete dynamic modulus master curve using the GFMM as presented in Section “Model determination from dynamic modulus test measurements” was performed in Katicha and Flintsch (2011). It was found that a GFMM comprising two fractional Maxwell elements was needed to provide an accurate representation of the storage modulus, loss modulus, and phase angle master curves.

We illustrate the construction of the master curve for uniaxial dynamic modulus tests performed at five different temperature levels (−10°C, 4.4°C, 21.1°C, 37.8°C, and 54.4°C) and six different frequencies (0.1, 0.5, 1, 5, 10, and 25 Hz). Test results for the storage and loss moduli are shown in Fig. 1. The resulting storage modulus and loss modulus master curves (reference temperature of 21.1 °CC) presented in Fig. 2 show good agreement between the fractional viscoelastic model and experimental data. Model parameters and shift factors are provided in Table 1.

Determining the GFKM from the GFMM

From the GFMM, the relaxation modulus can be obtained using Eq. 7. To evaluate the creep compliance, conversion can be used to determine the GFKM. This conversion is obtained analytically and therefore is exact. In the case of a GFMM containing two fractional Maxwell elements, the GFKM parameters can be obtained as follows:

$$\lambda_1 = x_1^{1/\alpha}$$

$$\lambda_2 = x_2^{1/\alpha}$$

Where x_1 and x_2 are the roots of the second-degree polynomial

$$X^2 + BX + C = 0$$

$$B = \frac{[\tau_1^{-\alpha} (E_\infty + E_2) + \tau_2^{-\alpha} (E_\infty + E_1)]}{(E_\infty + E_1 + E_2)}$$

$$C = \frac{E_\infty \tau_1^{-\alpha} \tau_2^{-\alpha}}{(E_\infty + E_1 + E_2)}$$

and D_0 , D_1 , and D_2 are obtained as

$$D_0 = \frac{1}{(E_\infty + E_1 + E_2)}$$

$$\lambda_1^{-\alpha} D_1 + \lambda_2^{-\alpha} D_2 = D_0 [(\tau_1^{-\alpha} + \tau_2^{-\alpha}) - (\lambda_1^{-\alpha} + \lambda_2^{-\alpha})]$$

Table 1 GFMM parameters and time–temperature shift factors

α	Moduli (MPa)			Relaxation Times (sec)		Shift Factors [$\log_{10}(aT)$]				
	E_∞	E_1	E_2	τ_1	τ_2	−10°C	4.4°C	21.1°C	37.8°C	54.4°C
0.342	145	11,745	14,375	3.01E-06	0.0145	3.75	2.13	0	−1.74	−3.36

Table 2 GFKM parameters

α	Compliances (MPa ⁻¹)			Retardation times (s)	
	D_0	D_1	D_2	λ_1	λ_2
0.342	3.81E-05	2.52E-05	680	1.50E-05	1.14E04

$$D_0 + D_1 + D_2 = \frac{1}{E_\infty}$$

The GFKM parameters are presented in Table 2 while the creep compliance and relaxation modulus of the fractional viscoelastic model are presented in Fig. 3.

To verify the accuracy of the conversion of the GFMM to the GFKM, we compare the magnitude of the dynamic complex modulus calculated using the GFMM to the magnitude of the dynamic complex modulus calculated using the GFKM. The dynamic complex modulus of the GFKM can be obtained from the dynamic complex compliance using Eq. 51.

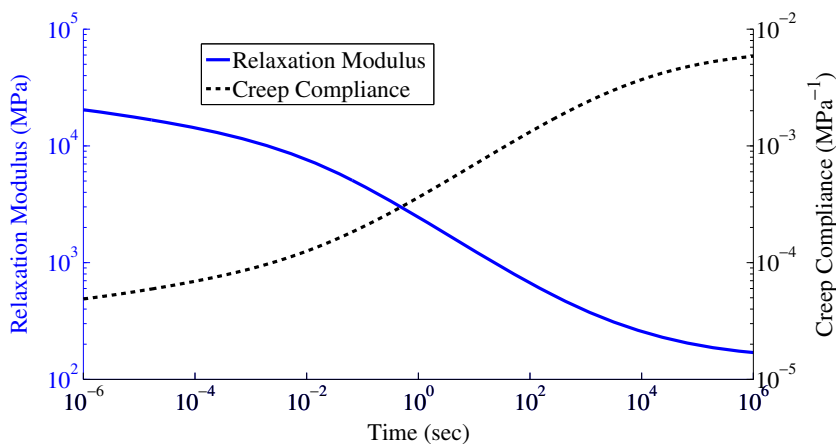
$$E^*(\omega) = \frac{1}{D^*(\omega)} \tag{51}$$

The metric used to evaluate the accuracy is:

$$M = \frac{|E_{GFMM}^*(\omega)| - |E_{GFKM}^*(\omega)|}{|E_{GFMM}^*(\omega)|} \tag{52}$$

The results were obtained using MATLAB. The calculation of M was performed for frequencies ranging from 10⁻⁵ to 10⁶ Hz, and the results are presented in Fig. 4. The values of M are of the order of 10⁻¹⁶, which is the order of error due to rounding in double precision floating point arithmetic.

Fig. 3 Relaxation modulus and corresponding creep compliance of the fractional viscoelastic model



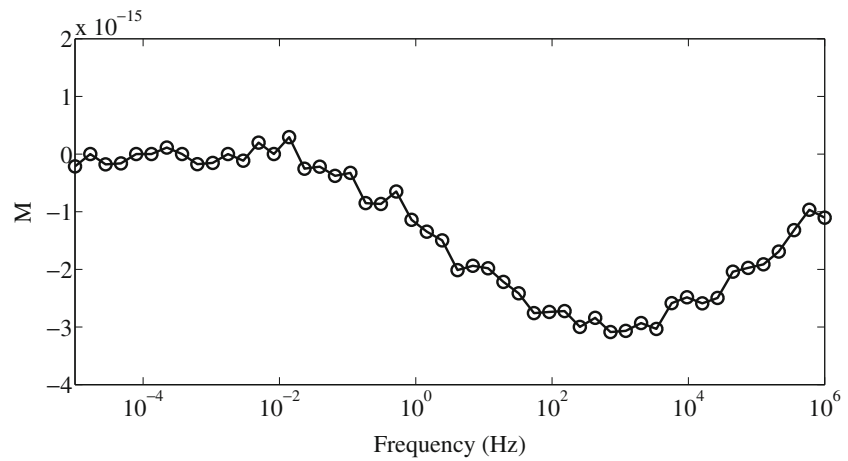
Continuous and discrete relaxation spectra

Equation 32 was used to obtain the relaxation spectrum of the GFMM. The relaxation spectrum is shown in Fig. 5. Because the GFMM comprises two fractional Maxwell elements, the relaxation spectrum is the sum of the relaxation spectra of each fractional Maxwell element. Note that the relaxation spectrum is completely defined by the GFMM, and therefore, it is obtained from the construction of the master curve.

The continuous relaxation spectrum can be discretized to obtain the discrete relaxation spectrum and Prony series parameters. Figure 6 shows the discretization of the relaxation spectrum for uniformly distributed relaxation times every one decade. Prony series parameters are equal to the individual rectangular areas under the discrete relaxation spectrum defined by the region of the constant relaxation spectrum.

As discussed earlier, the Prony series representation can be made arbitrarily close to either the GFMM or GFKM given appropriate values of c and δ . We first evaluate the effect of c , which is the largest relaxation time considered in evaluating the integral. Figure 7 shows the GFMM in the case $c \rightarrow \infty$ compared to the cases where $c = 10^2$ and $c = 10^6$ s. As larger relaxation times are considered, the approximation of the improper integral improves. Note that if we are only interested in the relaxation modulus at times less than 10² s, the approximation with $c = 10^6$ is reasonably accurate. This is due to the fact that the truncation error that is equal to the integral $\int_{c=10^6}^{\infty} [H(\xi)/\xi] \exp(-t/\xi) d\xi$ is relatively small compared to $g(t)$ for $t < 10^2$ s. The error term related to c is independent of the error term related to δ . That is, with c chosen, the Prony series expansion converges to the proper integral $\int_0^c [H(\xi)/\xi] \exp(-t/\xi) d\xi$ rather than the improper in-

Fig. 4 Accuracy of converting the GFMM to the GFKM evaluated using the metric of Eq. 52



tegral. This means that in the cases presented in Fig. 7, the Prony series expansion converges to the full curve (red color) for $c = 10^6$ s and to the dashed curve (green color) for $c = 10^2$ s.

The effect of δ on the accuracy of the discretization is presented in Fig. 8. In this example, the discretization is uniform on a logarithmic scale. To ensure that the error due to the approximation of the improper integral is negligible a value of $c = 10^{10}$ s was used. As seen in Fig. 8, relatively few numbers of Prony series parameters per decade are sufficient to provide a good approximation, with two parameters per decade giving excellent results. Furthermore, the convergence of the Prony series approximation is relatively fast. Figure 9 shows the percent error of the Prony series approximation. The largest percent error for one parameter per decade is less than 2% while that of two parameters per decade is less than 0.6%. However, it was found that the largest error for two parameters per decade is mainly due to c rather than the number of Prony series

parameters. Increasing c to 10^{16} s, the largest error for two-parameters-per-decade Prony series reduces to less than 0.03%. Note that Fig. 9 presents results of one parameter per decade instead of the one parameter per four decades presented in Fig. 8.

As mentioned earlier, the parameter c was set to 10^{10} s; this means that Prony series parameters with relaxation times up to 10^{10} s must be included in the series expansion. This results in a series with too many parameters. The Prony series can, however, be approximated as follows:

$$\begin{aligned}
 E(t) &= E_\infty + \sum_{i=1}^n C_i \exp(-t/\xi_i) \approx E_\infty + \sum_{i=m+1}^n C_i \\
 &\quad + \sum_{i=1}^m C_i \exp(-t/\xi_i) \\
 &= E_\infty + \sum_{i=1}^m C_i \exp(-t/\xi_i)
 \end{aligned}
 \tag{53}$$

Fig. 5 Continuous relaxation spectrum

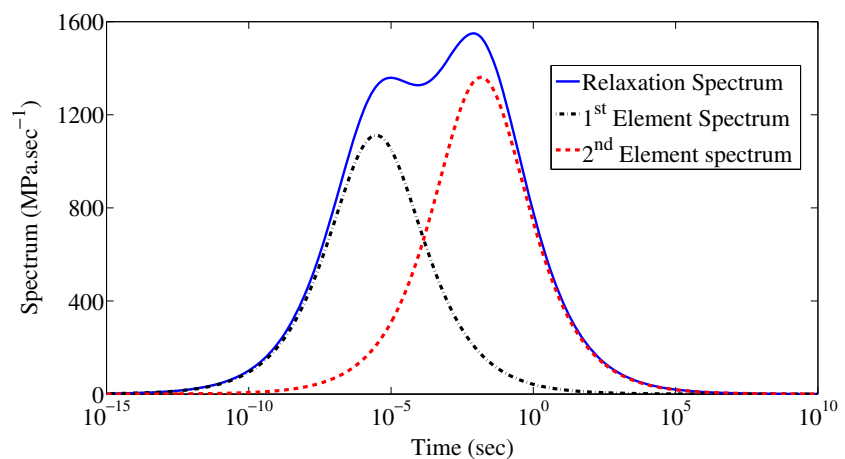


Fig. 6 Discrete relaxation spectrum

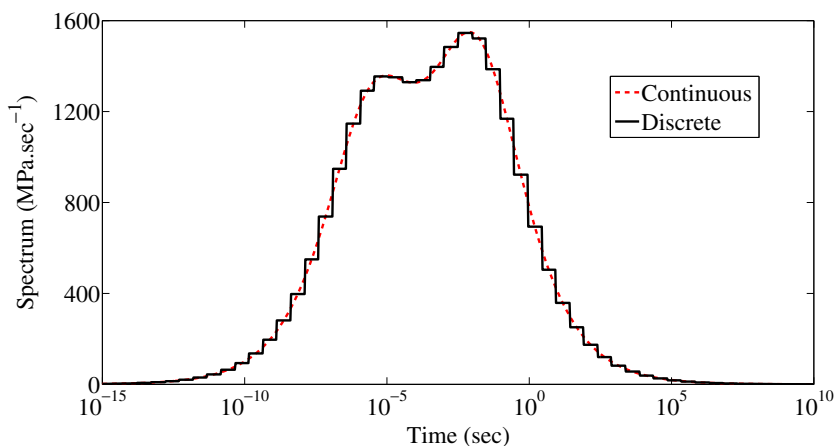


Fig. 7 Effect of c on the accuracy of the Prony series approximation

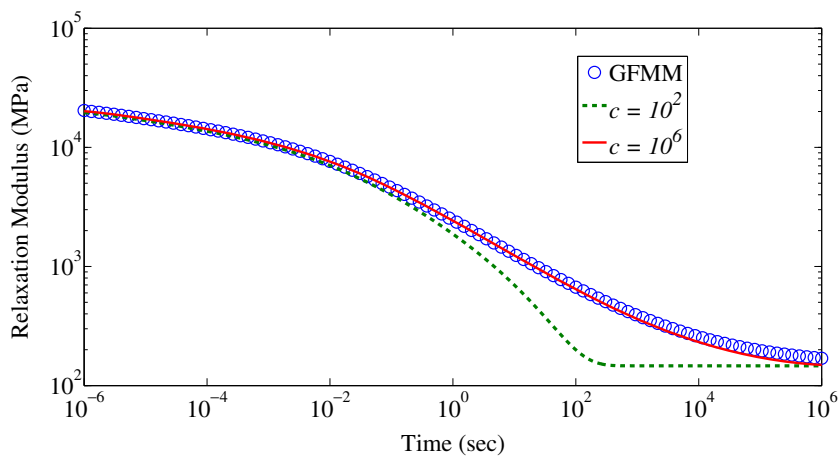


Fig. 8 Effect of δ on the Prony series approximation to the relaxation modulus. δ is measured on a logarithmic scale and equal to the inverse of the number of parameters per decade

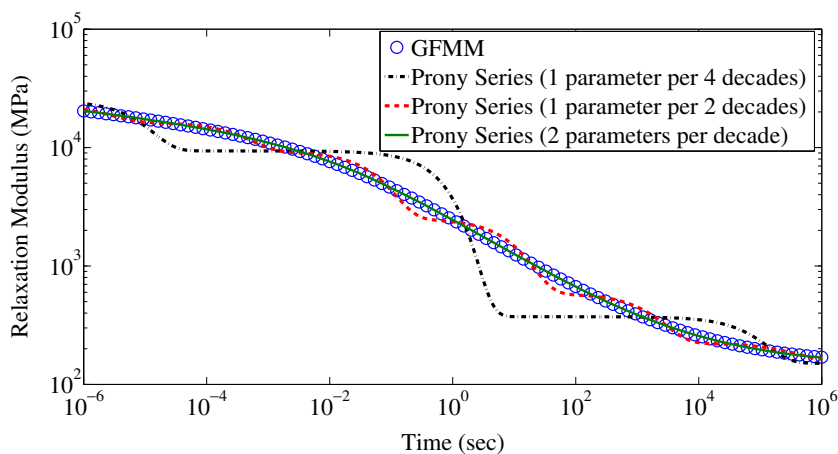
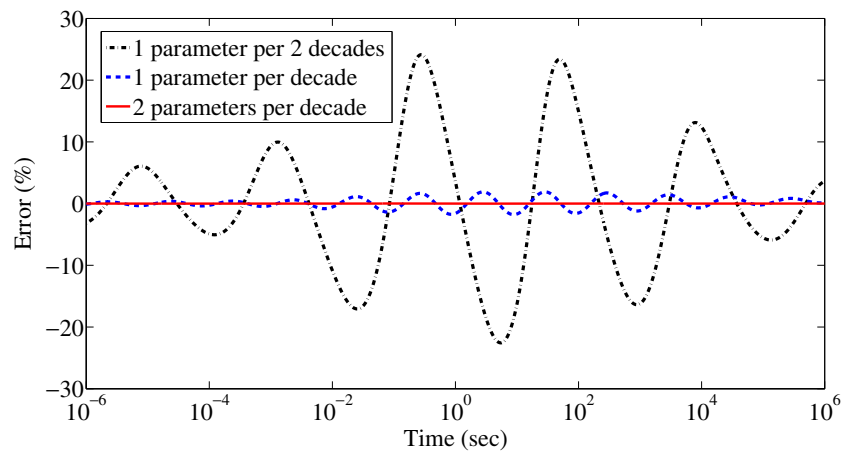


Fig. 9 Percent error of the Prony series approximation as a function of δ . δ is measured on a logarithmic scale and equal to the inverse of the number of parameters per decade



This approximation results from the fact that for $\xi_i \gg t$, $\exp(-t/\xi_i) \approx 1$. Therefore, Prony series parameters that have relaxation times much larger than the time range of interest can be omitted from the summation and directly added to the equilibrium modulus E_∞ . The resulting approximation error per parameter is about 10% for $t/\xi_i = 0.1$ and decreases to about 1% for $t/\xi_i = 0.01$.

Conclusion

This paper presents a comprehensive linear viscoelastic material characterization using fractional viscoelastic models. The advantage of this characterization is that constructing the master curve results in the complete linear viscoelastic characterization of the material. We have shown under which condition an analytical solution for interconversion between different viscoelastic functions of the fractional viscoelastic model can be obtained. Although numerical implementation of fractional viscoelastic models has proven difficult, we have shown that fractional viscoelastic models can be approximated to any desired level of accuracy using a Prony series expansion. This allows the numerical implementation of fractional viscoelastic models using efficient methods that have been developed for Prony series.

Acknowledgements We would like to acknowledge the anonymous reviewers for their comments and suggestions to improve the paper and for bringing to our attention an error in our initial definition of the Caputo derivative.

References

- Adolfsson K, Enelund M, Larsson S (2004) Adaptive discretization of fractional order viscoelasticity using sparse time history. *Comput Meth Appl Mech Eng* 193(42–44):4567–4590 doi:10.1016/j.cma.2004.03.006
- Adolfsson K, Enelund M, Olsson P (2005) On the fractional order model of viscoelasticity. *Mechanics of Time-dependent Materials* 9(1):15–34 doi:10.1007/s11043-005-3442-1
- Bagley RL, Torvik (1983) A theoretical basis for the application of fractional calculus to viscoelasticity. *J Rheol* 27(3):201–210 doi:10.1122/1.549724
- Baumgaertel M, Winter (1989) Determination of discrete relaxation and retardation time spectra from dynamic mechanical data. *Rheol Acta* 28(6):511–519 doi:10.1007/bf01332922
- Caputo M (1967) 4 Linear models of dissipation whose Q is almost frequency independent—II. *Geophys J Roy Astron Soc* 13(5):529–539 doi:10.1111/j.1365-246X.1967.tb02303.x
- Caputo M, Mainardi F (1971) Linear models of dissipation in anelastic solids. *Rivista Del Nuovo Cimento* 1(2):161–198 doi:10.1007/BF02820620
- Enelund M, Lesieutre (1999) Time domain modeling of damping using anelastic displacement fields and fractional calculus. *Int J Solids Struct* 36(29):4447–4472 doi:10.1016/S0020-7683(98), 00194-2
- Ford NJ, Simpson (2001) The numerical solution of fractional differential equations: speed versus accuracy. *Numer Algorithms* 26(4):333–346 doi:10.1023/A:1016601312158
- Friedrich C (1991) Relaxation and retardation functions of the Maxwell model with fractional derivatives. *Rheol Acta* 30(2):151–158 doi:10.1007/BF01134604
- Friedrich C, Braun H, Weese J (1995) Determination of relaxation time spectra by analytical inversion using a linear viscoelastic model with fractional derivatives. *Polym Eng Sci* 35(21):1661–1669 doi:10.1002/pen.760352102
- Glöckle WG, Nonnenmacher TF (1991) Fractional integral operators and Fox functions in the theory of viscoelasticity. *Macromolecules* 24(24):6426–6434. doi:10.1021/ma00024a009
- Haj Ali RM, Muliana (2004) Numerical finite element formulation of the Schapery non linear viscoelastic material model. *Int J Numer Methods Eng* 59(1):25–45 doi:10.1002/nme.861
- Henriksen M (1984) Nonlinear viscoelastic stress analysis—a finite element approach. *Comput Struct* 18(1):133–139 doi:10.1016/0045-7949(84), 90088-9

- Heymans N (1996) Hierarchical models for viscoelasticity: dynamic behaviour in the linear range. *Rheol Acta* 35(5):508–519 doi:[10.1007/BF00369000](https://doi.org/10.1007/BF00369000)
- Heymans N, Bauwens (1994) Fractal rheological models and fractional differential equations for viscoelastic behavior. *Rheol Acta* 33(3):210–219 doi:[10.1007/BF00437306](https://doi.org/10.1007/BF00437306)
- Honerkamp J, Weese J (1989) Determination of the relaxation spectrum by a regularization method. *Macromolecules* 22(11):4372–4377 doi:[10.1021/ma00201a036](https://doi.org/10.1021/ma00201a036)
- Honerkamp J, Weese J (1993) A nonlinear regularization method for the calculation of relaxation spectra. *Rheol Acta* 32(1):65–73 doi:[10.1007/bf00396678](https://doi.org/10.1007/bf00396678)
- Kaschta J, Schwarzl (1994) Calculation of discrete retardation spectra from creep data—I. Method. *Rheol Acta* 33(6):517–529 doi:[10.1007/bf00366336](https://doi.org/10.1007/bf00366336)
- Katicha SW, Flintsch (2011) Use of Fractional Order Viscoelastic Models to Characterize Asphalt Concrete. In: Proceedings of the 1st T&DI Congress, Chicago, IL, March 2011. ASCE, pp 677–687. doi:[10.1061/41167\(398\)65](https://doi.org/10.1061/41167(398)65)
- Koeller R (1984) Application of fractional calculus to the theory of viscoelasticity. *J Appl Mech* 51(2):299–307 doi:[10.1115/1.3167616](https://doi.org/10.1115/1.3167616)
- Koeller R (1986) Polynomial operators, Stieltjes convolution, and fractional calculus in hereditary mechanics. *Acta Mech* 58(3):251–264 doi:[10.1007/BF01176603](https://doi.org/10.1007/BF01176603)
- Lai J, Bakker A (1996) 3-D Schapery representation for nonlinear viscoelasticity and finite element implementation. *Comput Mech* 18(3):182–191 doi:[10.1007/BF00369936](https://doi.org/10.1007/BF00369936)
- Mainardi F (2010a) An historical perspective on fractional calculus in linear viscoelasticity. Arxiv preprint [arXiv:10072959](https://arxiv.org/abs/1007.2959)
- Mainardi F (2010b) Fractional calculus and waves in linear viscoelasticity: an introduction to mathematical models. Imperial College, London
- Mainardi F, Gorenflo R (2000) On Mittag-Leffler-type functions in fractional evolution processes. *J Comput Appl Math* 118(1–2):283–299 doi:[10.1016/S0377-0427\(00\)00294-6](https://doi.org/10.1016/S0377-0427(00)00294-6)
- Mainardi F, Spada G (2011) Creep, relaxation and viscosity properties for basic fractional models in rheology. *Eur Phys J Spec Top* 193(1):133–160
- Malkin (2006) The use of a continuous relaxation spectrum for describing the viscoelastic properties of polymers. *Polym Sci Series A* 48(1):39–45 doi:[10.1134/S0965545X06010068](https://doi.org/10.1134/S0965545X06010068)
- Mead D (1994) Numerical interconversion of linear viscoelastic material functions. *J Rheol* 38(6):1769–1795 doi:[10.1122/1.550526](https://doi.org/10.1122/1.550526)
- Oeser M, Freitag S (2009) Modeling of materials with fading memory using neural networks. *Int J Numer Methods Eng* 78(7):843–862 doi:[10.1002/nme.2518](https://doi.org/10.1002/nme.2518)
- Padovan J (1987) Computational algorithms for FE formulations involving fractional operators. *Comput Mech* 2(4):271–287 doi:[10.1007/BF00296422](https://doi.org/10.1007/BF00296422)
- Papoulia KD, Panoskaltis VP, Kurup NV, Korovajchuk I (2010) Rheological representation of fractional order viscoelastic material models. *Rheol Acta* 49(4):381–400 doi:[10.1007/s00397-010-0436-y](https://doi.org/10.1007/s00397-010-0436-y)
- Rossikhin YA, Shitikova MV (2010) Application of fractional calculus for dynamic problems of solid mechanics: novel trends and recent results. *Appl Mech Rev* 63(1):1–52 doi:[10.1115/1.4000563](https://doi.org/10.1115/1.4000563)
- Roy S, Reddy J (1988) A finite element analysis of adhesively bonded composite joints with moisture diffusion and delayed failure. *Comput Struct* 29(6):1011–1031 doi:[10.1016/0045-7949\(88\)90327-6](https://doi.org/10.1016/0045-7949(88)90327-6)
- Rudin W (1976) Principles of mathematical analysis. McGraw-Hill, New York
- Schiessel H, Blumen A (1995) Mesoscopic pictures of the sol-gel transition: ladder models and fractal networks. *Macromolecules* 28(11):4013–4019 doi:[10.1021/ma00115a038](https://doi.org/10.1021/ma00115a038)
- Schiessel H, Metzler R, Blumen A, Nonnenmacher T (1995) Generalized viscoelastic models: their fractional equations with solutions. *J Phys A Math Gen* 28(23):6567 doi:[10.1088/0305-4470/28/23/012](https://doi.org/10.1088/0305-4470/28/23/012)
- Sharma R, Cherayil (2010) Polymer melt dynamics: microscopic roots of fractional viscoelasticity. *Phys Rev E* 81(2):021804 doi:[10.1103/PhysRevE.81.021804](https://doi.org/10.1103/PhysRevE.81.021804)
- Stadler F, Bailly C (2009) A new method for the calculation of continuous relaxation spectra from dynamic-mechanical data. *Rheol Acta* 48(1):33–49 doi:[10.1007/s00397-008-0303-2](https://doi.org/10.1007/s00397-008-0303-2)
- Taylor RL, Pister KS, Goudreau (1970) Thermomechanical analysis of viscoelastic solids. *Int J Numer Methods Eng* 2(1):45–59 doi:[10.1002/nme.1620020106](https://doi.org/10.1002/nme.1620020106)
- Weese J (1993) A regularization method for nonlinear ill-posed problems. *Comput Phys Commun* 77(3):429–440 doi:[10.1016/0010-4655\(93\)90187-h](https://doi.org/10.1016/0010-4655(93)90187-h)